NANO LETTERS

2009
Vol. 9, No. 6
2260-2266

Precise Semiconductor Nanowire Placement Through Dielectrophoresis

Sourobh Raychaudhuri, Shadi A. Dayeh, Deli Wang, and Edward T. Yu*

Department of Electrical and Computer Engineering, University of California, San Diego, La Jolla, California 92093

Received February 9, 2009; Revised Manuscript Received April 14, 2009

ABSTRACT

We demonstrate the ability to precisely control the alignment and placement of large numbers of InAs nanowires from solution onto very narrow, prepatterned electrodes using dielectrophoresis. An understanding of dielectrophoretic behavior associated with such electrode geometries is essential to development of approaches for assembly of intricate nanowire systems. The influence of signal frequency and electrode design on nanowire manipulation and placement is examined. Signal frequencies in the range of 10 MHz are found to yield high percentages of aligned nanowires on electrodes with dimensions similar to that of the nanowire. Strategies for further improvement of nanowire alignment are suggested and analyzed.

Nanowires, by virtue of their one-dimensional geometry and unique possibilities for engineering of electronic and optical properties, hold great promise for a variety of device applications including chemical and biological sensors,[1,2] field effect transistors,[3,4] light-emitting diodes,[5] lasers,[6] and photodetectors.[7,8] Furthermore, nanowires can be synthesized through a variety of techniques,[9,10] some of which allow for unique device geometries, such as axial or coaxial heterostructures, that are not easily realized in planar device fabrication schemes.[11]

However, while significant advances have been made in nanowire synthesis and device characterization, postgrowth manipulation and placement of nanowires in a coherent and useful fashion continues to be a considerable challenge, one that must be overcome to realize large-scale complex nanowire based systems. A number of schemes have been proposed to meet this challenge and include the use of Langmuir−Blodgett films,[12] fluidic directed assembly,[13] dry-transferprinting,[14]anddielectrophoresis(DEP).[15−21]Langmuir−Blodgett techniques, fluidic directed assembly, and dry-transfer printing all offer the ability to line up nanowires in parallel but do not allow for precise nanowire placement for functional systems.

Dielectrophoresis, which refers to the use of AC electric fields to manipulate neutrally charged particles in solution,[22] offers another method to attract nanowires onto predefined electrodes. DEP can be tailored to work with nanowires of various conductivities and materials and allows for integration upon arbitrary substrates including those that require low temperature processing such as flexible substrates. Furthermore, because nanowires are placed on predefined electrodes identifying their final location, integrating them with a larger system becomes straightforward. DEP also allows the added flexibility of integrating several different types of nanowires into one system by performing a series of DEP steps.

To fully realize these capabilities, DEP must be carefully controlled to ensure that wires are placed precisely at desired locations, and only at desired locations. To this end it is necessary to determine the relevant parameters that affect DEP and how to control them. Earlier DEP studies have utilized DC and AC voltages to align nanowires onto predefined electrodes in order to study their properties.[15−21] These studies employed electrode structures ranging in size from several micrometers to tens of micrometers to demonstrate DEP alignment of nanowires. Such electrodes are useful for constructing proof-of-concept devices but not necessarily sufficient to build complex nanowire systems. To realize such systems through DEP, it will be necessary to use more intricate electrode structures, and consequently the electrostatics associated with such structures must be understood. More recently, a combined integration scheme using DEP, capillary forces, and nanowire lift-off has been used to construct nanowire resonators and sensors at specified locations.[23,24] In these works, the authors use relatively large electrodes on which alignment sites are defined lithographically in photoresist, to achieve very precise placement of nanowires. Such a scheme is shown to be effective and can be utilized for any nanowire system where a large number of identical nanowires are to be placed in parallel. Much of the promise of nanotechnology lies in the ability to integrate different functional building blocks into a single system. To construct systems where different species of nanowires are

* To whom correspondence should be addressed. E-mail: ety@ece.ucsd.edu.

10.1021/nl900423g CCC: $40.75
Published on Web 05/06/2009

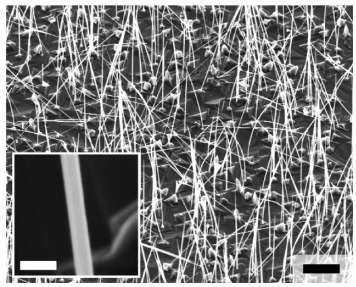

Figure 1. SEM image of as grown InAs nanowires before suspension. Scale bar is 10 μm for figure, 200 nm for inset.

placed near each other in a series of DEP steps, it will be necessary to use individually addressable, and typically narrow, fingerlike electrodes at each alignment site. In such a scheme, it would be possible to power specific alignment sites, attract nanowires to those sites and only those sites without attracting wires to the lines used to power those sites, or to other areas of the chip. To accomplish this level of control, it is necessary to understand the electrostatics associated with intricate electrodes that have physical dimensions similar to that of the nanowire and how such electrodes may differ in DEP alignment behavior from the larger electrode structures discussed in previous works. In this letter, we demonstrate the ability to precisely control the alignment and placement of semiconductor nanowires from solution onto prepatterned narrow electrode structures using DEP. We examine and analyze the importance of a number of physical parameters and conclude that higher signal frequencies and careful electrode design will allow for precise nanowire alignment on very narrow electrodes.

The InAs nanowires used in these studies were grown by metal-organic chemical vapor deposition.[25] Au particles (40 nm) were randomly dispersed from solution across the surface of an n-InAs (111)B substrate for seeding nanowire growth. The growth was carried out for 40 min in a horizontal chamber at 500 °C under 100 Torr chamber pressure using trimethylindium and arsine in H_2 carrier gas at an input V/III ratio of 64. The resulting nanowires have average diameters of ~150 nm and lengths of ~20 μm with a representative image of as grown nanowires shown in Figure 1. The grown nanowires were suspended into 150 μL of deionized water (resistivity = 18.2 MΩ-cm) by sonication for 7 s. After suspension, the nanowire lengths are between 12 and 20 μm.

Electrodes were constructed using standard microfabrication techniques in order to serve as a framework on which to align the suspended nanowires. An insulating substrate was first prepared using plasma-enhanced chemical vapor deposition (PECVD) to deposit 500 nm of SiN_x on an n-Si (100) substrate. Metal alignment electrode arrays consisting of 10 nm Ti/90 nm Au were then fabricated using e-beam lithography and e-beam evaporation followed by a standard lift-off procedure. Each electrode array contained a set of alignment sites, each of which has two fingers, 1 μm wide and either 20 or 45 μm in length with a 10 μm gap between them, as shown in Figure 2. PECVD was then used to deposit 250 nm SiO_2 over the entire metal structure. E-beam lithography followed by a wet etch in buffered oxide etch

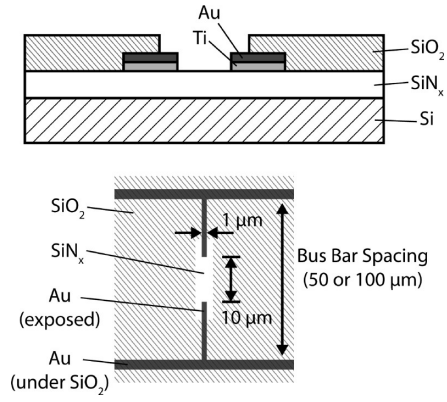

Figure 2. Schematic diagram of electrode layer structure (top) and top-view of alignment site (bottom).

(BOE) was then carried out to remove the oxide layer at each alignment site. Electrode arrays were fabricated in groups of 50 alignment sites with 100 μm spacing between bus bars or 100 alignment sites with 50 μm spacing between bus bars.

Six different DEP electrode array structures (DEP chips) were employed in our experiments. Three of them contained 100 alignment sites with 50 μm bus bar spacing while the other three contained 50 alignment sites with 100 μm bus bar spacings. In each of the six experiments, a micropipet was used to apply 2 μL of nanowire solution to the surface of the DEP chip, completely covering all available alignment sites. An HP33120A function generator was used to apply a voltage signal, $V(t) = V_{ac} \sin(\omega t)$, where $V_{ac} = 5$ V and ω corresponds to a signal frequency of either 10 kHz, 1 or 10 MHz. After precisely 3 min, dry nitrogen was used to blow the 2 μL drop of solution off of the chip. Once the drop was removed, the AC signal was turned off and the chips were examined using optical and scanning electron microscopy.

Optical and SEM images revealed that the vast majority of wires left behind after drop removal were in physical contact with a metal electrode at an alignment site. Wires that were not in contact with an electrode were swept away when the drop was blown off by N_2 gas. The wires that were in contact either bridged the alignment site gap, as shown in Figure 3a−c, or only had contact with one of the two alignment fingers, as shown in Figure 3c,d. Figure 3c indicates that it is possible to have both bridging and nonbridging events at the same alignment site. Wires that bridge the gap at alignment sites (as shown in Figure 3a−c) will be referred to hereafter as precisely aligned wires. Wires that are only in contact with one finger at an alignment site (as shown in Figure 3c,d) will be referred to as unaligned wires.

Wires that were successfully aligned (as shown in Figure 3a−c) did not immediately make electrical contact with alignment electrodes. This is likely due to a thin layer of oxide that is believed to form on the surface of the InAs nanowire after removal from the growth chamber. In order to make ohmic contact to InAs nanowires, a BOE dip is typically required to remove the oxide.[3,4] To verify this, three alignments sites with a total of four aligned wires between

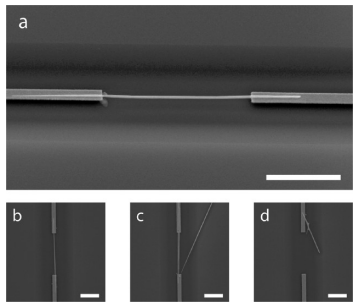

Figure 3. SEM images of individual alignment sites after DEP alignment. SEM image of a precisely aligned nanowire taken at 45° (a) and from directly overhead (b). SEM image of an alignment site with both an aligned and unaligned nanowire (c). SEM image of an alignment site with only an unaligned nanowire (d). Scale bar is 5 μm for all images.

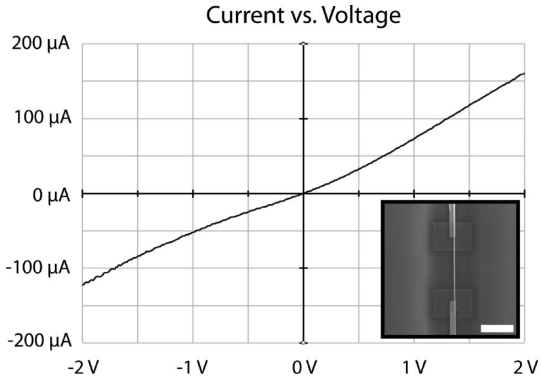

Figure 4. *IV* curve for four aligned nanowires in parallel suggesting each nanowire has a total resistance of approximately 60 kΩ. Inset shows one of the four aligned nanowires with postalignment metallization. Scale bar for inset is 5 μm.

them were chosen at random, and metal contacts were patterned over the tips of the aligned nanowires. E-beam lithography was used to define the contact areas. A 30 s wet oxide etch (in BOE) immediately followed by e-beam evaporation and lift-off was used to pattern metal contacts (15 nm Ti/90 nm Al) over the nanowire and electrode tips. The measured *IV* curve, shown in Figure 4, suggests that each nanowire has a resistance of approximately 60 kΩ and demonstrates that the InAs nanowires maintain their electrical properties through the alignment process and yield resistances similar to those reported in the literature.[26]

Figure 5 shows optical microscope images of each DEP chip after the alignment experiment. The top row shows three chips with 100 alignment sites (and 50 μm bus bar spacing) that were driven at 10 kHz, 1 MHz, and 10 MHz, respectively. The second row contains images of three chips with 50 alignment sites (and 100 μm bus bar spacing) that were also driven at 10 kHz, 1 MHz, and 10 MHz, respectively. Sites with perfect alignment are indicated by a rectangle and wires that were attracted to alignment sites, but were not aligned, are highlighted with a thick line to improve their visibility in the figure. Figure 6 shows a histogram of the percentage of alignment sites that attracted nanowires. Each histogram bar is broken into portions showing the percentage of sites that attracted only perfectly aligned wires, only unaligned wires, and both aligned and unaligned wires. From Figures 5 and 6, we note that the percentage of alignment sites that attracted nanowires increases slightly as the frequency is increased from 10 kHz to 1 MHz and then drops off as frequency is further increased to 10 MHz. The increase in the total number of attracted wires from 10 kHz to 1 MHz is likely due to a reduced influence from electro-fluidic effects in aqueous solution[27] (such as electro-osmosis and double layer screening) allowing DEP to become a more dominant force in the system. The reduction in the total number of attracted wires from 1 to 10 MHz is likely due to the reduced DEP force as a function of frequency that is expected in the commonly accepted DEP theory and will be discussed in detail in the next paragraph. Figure 6 also reveals that as frequency is increased the percentage of attracted wires that are perfectly aligned increases. This might initially seem counterintuitive; because DEP force is used to both attract and align wires one might expect that weaker DEP forces at higher frequencies should result in a lower percentage of attracted wires being perfectly aligned. The reason this does not occur has to do with the nature of DEP force on an anisotropic particle such as a nanowire.

The translational dielectrophoretic force on a spheroid is given by the well-known analytical expression[22]

$$F_{\mathrm{DEP}} = c\varepsilon_{\mathrm{m}}\mathrm{Re}[f_{\mathrm{cm}}]\nabla E^2 \tag{1}$$

where c represents a prefactor containing information about the volume of the particle, ε_{m} represents the permittivity of the medium, E represents the magnitude of the electric field, and f_{cm} is the Clausius−Mossotti factor, which is a measure of the strength of a dipole that can be induced in a particle through the presence of an external field. The Clausius−Mossotti factor contains information about the permittivities of both the medium (in this case deionized water) and the InAs nanowire as well as the signal frequency. Equation 1 is valid for an isotropic spheroid. It has been shown that a prolate spheroid serves as a reasonable approximation for a cylindrical particle with a high aspect ratio[28] and thus allows the use of analytical expressions to examine the DEP force on nanowire. For a prolate spheroid, f_{cm} will be a different function for each axis of the particle. As a result, to compute the total DEP force acting on a particle, the electric field gradient vector must be broken down into components to determine the magnitude of the DEP force along each axis of the nanowire. In situations where the field gradient is oriented parallel to the nanowire, the DEP force will only have a single component aligned along the length of the nanowire. As a result only the Clausius−Mossotti factor along the long axis of the nanowire must be considered to calculate the magnitude of the translational DEP force and is given by[22]

$$f_{\mathrm{cm(longaxis)}} = \frac{\varepsilon_{\mathrm{p}}^* - \varepsilon_{\mathrm{m}}^*}{\varepsilon_{\mathrm{m}}^*} \tag{2}$$

where the subscripts p and m denote properties of the particle and medium, respectively, and ε^* is the complex permittivity given by

$$\varepsilon^* = \varepsilon - j\frac{\sigma}{\omega} \tag{3}$$

where σ and ε are the conductivity and permittivity, respectively, of the material in question and ω represents

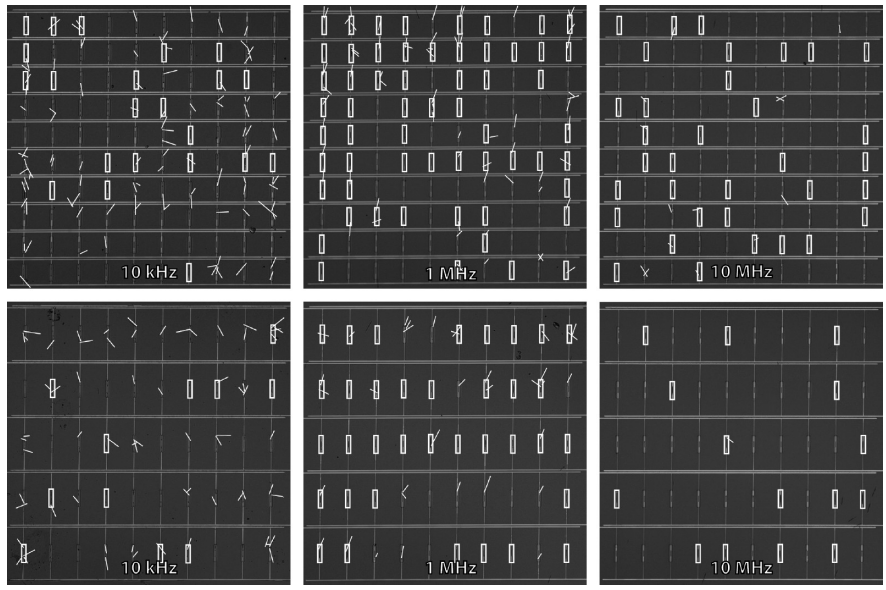

Figure 5. Optical microscope images of electrode arrays after DEP alignment. The top and bottom rows show images of chips with 100 alignment sites and 50 alignment sites, respectively. Sites with perfect alignment are indicated by a rectangle while unaligned wires are indicated by a line. Each image is 500 × 500 μm.

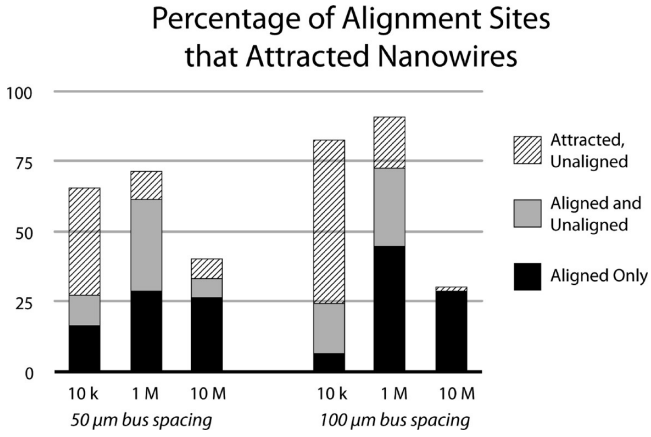

Figure 6. Histogram showing the percentage of alignment sites that attracted nanowires. Each bar is divided to show the percentage of sites that attracted and perfectly aligned a nanowire (black), sites that attracted and perfectly aligned a nanowire while others remained unaligned at the same site (gray), and sites that attracted but did not align nanowires (lines).

the signal frequency. In situations where the gradient of the electric field is perfectly perpendicular to the nanowire the DEP force will only have a single component perpendicular to the long axis of the nanowire. As a result when computing the magnitude of the DEP force it is only necessary to consider the Clausius−Mossotti factor along the short axis of the nanowire, which is given by[22]

$$f_{\mathrm{cm(shortaxis)}} = 2\frac{\varepsilon_{\mathrm{p}}^{*} - \varepsilon_{\mathrm{m}}^{*}}{\varepsilon_{\mathrm{p}}^{*} + \varepsilon_{\mathrm{m}}^{*}} \tag{4}$$

In cases where the gradient is neither parallel nor perpendicular to the nanowire, it is necessary to consider the effect of both the short-axis and long-axis Clausius−Mossotti factors in order to compute the magnitude and direction of the DEP force.

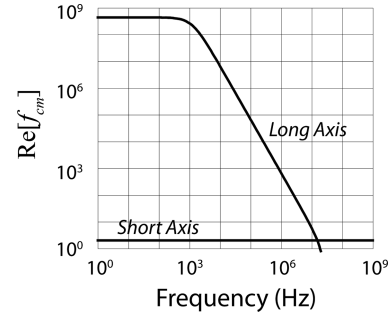

Figure 7. Calculated values for the real part of the Clausius−Mossotti factor for the long and short axes of an InAs nanowire ($\varepsilon_{\mathrm{p}} = 12.3$, $\sigma_{\mathrm{p}} = 6.4 \times 10^3$ S/m) suspended in deionized water ($\varepsilon_{\mathrm{m}} = 80$, $\sigma_{\mathrm{m}} = 1 \times 10^{-6}$ S/m) plotted as a function of AC signal frequency.

Figure 7 shows the value for the real part of the Clausius−Mossotti factor along the long and short axis of the nanowire as a function of frequency for an InAs nanowire ($\varepsilon_{\mathrm{p}} = 12.3$, $\sigma_{\mathrm{p}} = 6.4 \times 10^3$ S/m) suspended in deionized water ($\varepsilon_{\mathrm{m}} = 80$, $\sigma_{\mathrm{m}} = 1 \times 10^{-6}$ S/m). From Figure 7, it is clear that at low frequencies the DEP force will be dominated by the long-axis component resulting in a very strong force along the length of the nanowire. At higher frequencies, the dominance of the long-axis Clausius−Mossotti factor becomes less significant.

Figure 8 illustrates this point by showing plots of the calculated direction and magnitude of the resulting DEP force as a function of the electric field gradient orientation with respect to the nanowire orientation at different signal frequencies. At low frequencies, the DEP force is expected to be large and dominated by the long axis Clausius−Mossotti factor. As a result nanowires will tend to move along the electric field lines at lower frequencies, whereas at higher frequencies the dominance of the long axis Clausius−Mossotti factor is reduced, resulting in wires experiencing a translational force that is more along the gradient of the electric

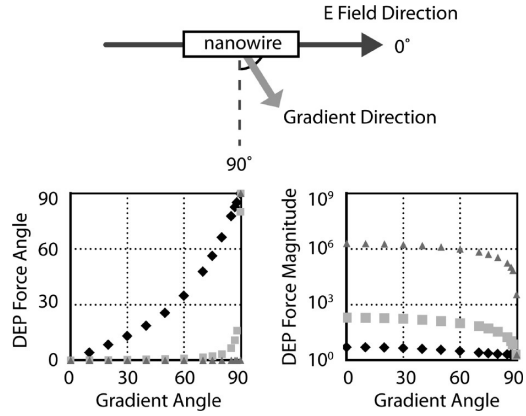

Figure 8. Diagram of a nanowire in an electric field pointing to the right with an arbitrary electric field gradient (top). DEP force angle and relative force magnitude are plotted as a function of gradient direction angle for signal frequencies of 10 kHz (triangles), 1 MHz (squares), and 10 MHz (diamonds).

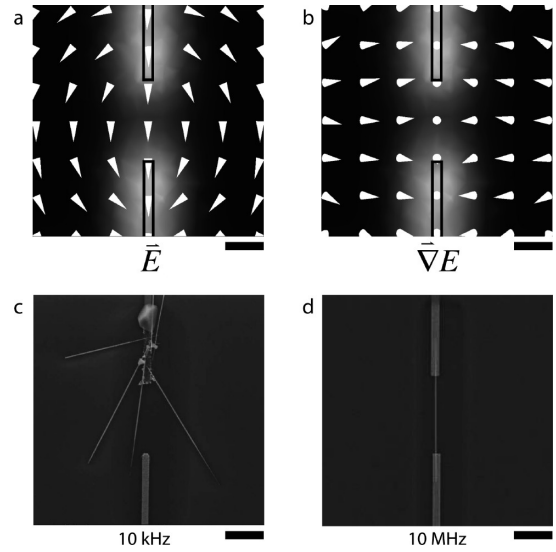

Figure 9. (a,b) Both show finite element simulation results 5 μm above an alignment site. The white arrows represent the electric field direction (a) and electric field gradient direction (b). The coloring of both (a) and (b) represent the magnitude of the gradient vector squared (which corresponds to DEP force magnitude) on a linear scale where lighter shading indicate a greater value. (c,d) SEM images of representative alignment sites at signal frequencies of 10 kHz and 10 MHz, respectively. Scale bars are 5 μm for all images.

field. Figures 7 and 8 show that at lower frequencies the total magnitude of the DEP force will be large, but as frequency increases, the total DEP force decreases resulting in the reduced nanowire attraction yield observed at 10 MHz.

The increased alignment observed among attracted nanowires at high frequencies can be explained as a consequence of the nature of the gradient and electric field direction around narrow electrode structures. As frequency is increased nanowires are less inclined to move strictly in the direction of the electric field and move more along the direction of the gradient. Because of this, nanowires are less likely to be drawn to a single electrode finger and more likely to bridge the gap between electrodes. In order to illustrate this, three-dimensional finite element analysis using the COMSOL software package was employed to calculate the electric field and field gradient near an alignment site. Figure 9a,b shows the resulting calculations for electric field direction, electric field gradient, and magnitude of the electric field gradient squared immediately around an alignment site 5 μm above the alignment electrodes. Because the gradient of the electric field drops off quickly with distance from the electrode it should be noted that the DEP force acts primarily on wires that are already close to an alignment site. From Figure 8, we recall that at low frequencies such wires will follow the electric field lines back to one of the two electrodes at an alignment site, whereas at higher frequencies such wires will follow the gradient and be more likely to contact both electrodes at an alignment site. Thus, at lower frequencies we would expect to find more wires that are only touching one of the two electrodes at an alignment site, whereas at higher frequencies we would expect to observe a greater percentage of wires bridging the gap.

Inspection of the SEM images in Figure 9c,d and the optical images in Figure 5 reveals that at higher frequencies most of the collected wires are precisely aligned, whereas at lower frequencies a large fraction of the collected wires are only in contact with one of the electrodes at an alignment site. From these experiments and analysis, it is clear that choice of frequency is very important in achieving precision alignment on fine electrode structures. In larger structures, it is easier to take advantage of the long-axis Clausius−Mossotti factor to draw in nanowires that will already be approximately aligned in the desired orientation. For finer structures the long-axis Clausius−Mossotti factor will draw wires to a single electrode and align them in a radial pattern, and thus it is necessary to select a frequency where the short-axis force has enough influence to draw the wire along the gradient to position the nanowire such that it will bridge the gap between electrodes.

Because the electric field gradient drops off quickly with distance from the electrode, to achieve precision alignment it is necessary for wires to be free to move sufficiently close to an alignment site so that they will come under its influence and be aligned. To this end, it is important to consider the macroscopic electrode structure used to organize alignment sites. To elucidate this issue, we conducted experiments with both single and double bus bar structures for the electrode arrays. In the latter, the bus bar consists of both a positive signal and a ground signal that are very close together, as shown in Figure 10a. Figure 10 shows a comparison of alignment attempts at a moderate frequency of 1 MHz for both the double bus bar and single bus bar structure (where a much greater distance separates the positive and ground signals). It is clear that precision alignment is more successful in the double bus bar structure, and that nanowires are more likely to be attracted directly to the bus bars in the single bus bar structure. This is because the electric field gradient from the double bus bar, while very great immediately around the bus bar itself, drops off more quickly with distance making the double bus bar less visible to wires that might be floating above an alignment site. The electric field gradient

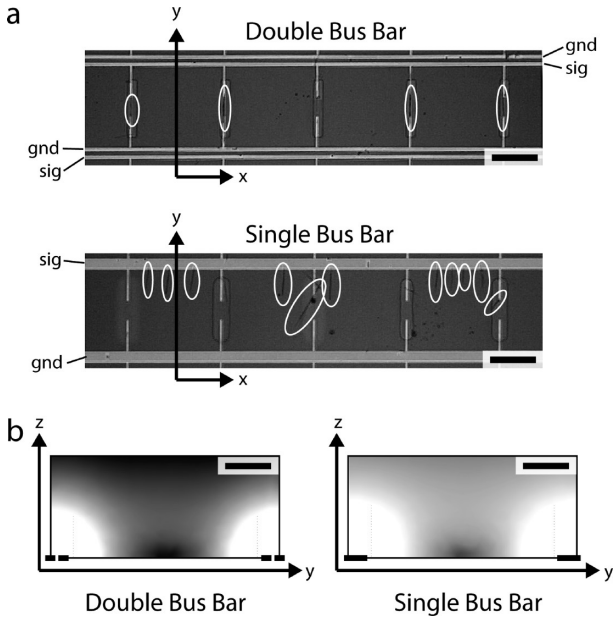

Figure 10. (a) Optical microscope images of five alignment sites in both double and single bus bar architectures after DEP alignment. Circles indicate nanowire positions after alignment attempt. (b) Results of finite element simulations for the gradient of the electric field squared (which corresponds to DEP force magnitude) on a logarithmic scale where lighter shading indicate a greater value. The simulation is for a cross-sectional plane directly between two alignment sites as indicated by the location of the axis in the images in (a). Scale bars are 25 μm for (a) and 10 μm for (b).

in the single bus bar structure drops off much more slowly with distance and is thus able to influence and attract wires that are further away and may be above the alignment site, pulling them down to the bus bar and preventing precision alignment.

The double and single bus bar electrodes were modeled using three-dimensional finite element simulations to illustrate the differing nature of the electric field and field gradients of these two electrode geometries. Figure 10b shows a cross section of the magnitude of the electric field gradient squared as a function of position in the region between two alignment sites and above the surface of the electrode array (the *y*-*z* plane). The lighter regions shown in the single bus bar case in the area directly between the bus bars suggest that wires in this region will be influenced by a mild, but relevant DEP force drawing them toward the bus bars. The DEP force in this region, while small, is expected to be about 1 order of magnitude greater than in the double bus bar case. Thus, in the single bus bar case, it is expected that a wire floating as close as 20 μm above an alignment site is still likely to come under the influence of the electric field of the single bus bar, and move toward it, rather than to be influenced and drawn into an alignment site. This is consistent with experimental observations, which show the single bus bar geometry does not allow for precision alignment in the way the double bus bar geometry does but rather results in wires being collected at the bus bars.

In summary, we have shown that DEP is a viable approach for placing a relatively large number of wires with a high level of precision on fine electrode structures by paying careful attention to the signal frequency as well as the macroscopic electrode architecture that is employed. While these studies showed reasonable alignment yields for InAs nanowires in deionized water, the observed trends can be used as a guide to determine optimal signal conditions for precise alignment on intricate electrode structures for a variety of nanowire suspensions. In our experiment, better than 70% of alignment sites saw precise alignment at moderate frequencies, but with a large number of unaligned wires at alignment sites throughout the structure. At higher frequencies 30% of alignment sites attracted nanowires almost all of which experienced precise alignment. Because the magnitude of the total DEP force is reduced at higher frequencies, it is believed that the high frequency yields can be further improved by attaining tighter control over the uniformity and density of wires in suspension in order to increase the likelihood that a nanowire will come under the influence of an alignment site and achieve perfect alignment.

Acknowledgment. The authors would like to thank Arthur Zhang and Jung Park for their assistance with SEM imaging. The authors of this work would like to acknowledge financial support from the National Science Foundation (ECS 0506902).

References

(1) Cui, Y.; Wei, Q.; Park, H.; Lieber, C. M. *Science* **2001**, *293*, 1289.
(2) Hsueh, T. J.; Chang, S. J.; Hsu, C. L.; Lin, Y. R.; Chen, I. C. *Appl. Phys. Lett.* **2007**, *91*, 053111.
(3) Dayeh, S. A.; Soci, C.; Yu, P. K. L.; Yu, E. T.; Wang, D. *Appl. Phys. Lett.* **2007**, *90*, 162112.
(4) Thelander, C.; Fröberg, L. E.; Rehnstedt, C.; Samuelson, L; Wernersson, L.-E. *IEEE Elect. Dev. Lett.* **2008**, *29*, 206.
(5) Svensson, C. P. T.; Mårtensson, T.; Trägårdh, J.; Larsson, C.; Rask, M.; Hessman, D.; Samuelseon, L.; Ohlsson, J. *Nanotechnology* **2008**, *19*, 305201.
(6) Zhou, H.; Wissinger, M.; Fallert, J.; Hauschild, R.; Stelzl, F.; Klingshirn, C.; Kalt, H. *Appl. Phys. Lett.* **2007**, *91*, 181112.
(7) Soci, C.; Zhang, A.; Xiang, B.; Dayeh, S. A.; Aplin, D. P. R.; Park, J.; Bao, X. Y.; Lo, Y. H.; Wang, D. *Nano Lett.* **2007**, *7*, 1003.
(8) Novotny, C. J.; Yu, E. T.; Yu, P. K. L. *Nano Lett.* **2008**, *8*, 775.
(9) Wagner, R. S.; Ellis, W. C. *Appl. Phys. Lett.* **1964**, *4*, 89.
(10) Motohisa, J.; Noborisaka, J.; Takeda, J.; Inari, M.; Fukui, T. *J. Cryst. Growth* **2004**, *272*, 180.
(11) Lu, W.; Lieber, C. M. *J. Phys. D: Appl. Phys.* **2006**, *39*, R387.
(12) Whang, D.; Jin, S.; Wu, W.; Lieber, C. M. *Nano Lett.* **2003**, *3*, 1255.
(13) Huang, Y.; Duan, X.; Wei, Q.; Lieber, C. M. *Science* **2001**, *291*, 630.
(14) Javey, A.; Nam, S.; Friedman, R. S.; Yan, H.; Lieber, C. M. *Nano Lett.* **2007**, *7*, 773.
(15) Lee, S. Y.; Hyung, J. H.; Lee, S. K. *Electron. Lett.* **2008**, *44*, 695.
(16) Lee, J.-W.; Moon, K.-J.; Han, M.-H.; Myoung, J.-M. *Solid State Commun.* **2008**, *148*, 194.
(17) Ingole, S.; Aella, P.; Hearne, S. J.; Picraux, S. T. *Appl. Phys. Lett.* **2007**, *91*, 033106.
(18) Liu, Y.; Chung, J.-H.; Liu, W. K.; Ruoff, R. S. *J. Phys. Chem. B* **2006**, *110*, 14098.
(19) Kim, T. H.; Lee, S. Y.; Cho, N. K; Seong, H. K.; Choi, H. J.; Jung, S. W.; Lee, S. K. *Nanotechnology* **2006**, *17*, 3394.
(20) Motayed, A.; He, M.; Davydov, A. V.; Melngailis, J.; Mohammad, S. N. *J. Appl. Phys.* **2006**, *100*, 114310.
(21) Evoy, S; DiLello, N.; Deshpandae, V.; Narayanan, A.; Liu, H.; Riegelman, M.; Martin, B. R.; Hailer, B.; Bradley, J.-C.; Weiss, W.; Mayer, T. S.; Gogotsi, Y.; Bau, H. H.; Mallouk, T. E.; Raman, S. *Microelectron. Eng.* **2004**, *75*, 31.
(22) Jones, T. B. *Electromechanics of Particles*; Cambridge University Press: New York, NY, 1995.
(23) Li, M.; Bhiladvala, R. B.; Morrow, T. J.; Sioss, J. A.; Lew, K.-K.; Redwing, J. M.; Keating, C. D.; Mayer, T. S. *Nat. Nanotechnol.* **2008**, *3*, 88.

(24) Morrow, T. J.; Li, M.; Kim, J.; Mayer, T. S.; Keating, C. D. *Science* **2009**, *323*, 352.
(25) Dayeh, S. A.; Yu, E. T.; Wang, D. *Nano Lett.* **2007**, *7*, 2486.
(26) Dayeh, S. A.; Susac, D.; Kavanagh, K. L.; Yu, E. T.; Wang, D. *Adv. Func. Mat.* [Online early access]. DOI: 10.1002/adfm.200801307. Published online: 2009 .
(27) Morgan, H.; Green, N. G. *AC Electrokinetics: colloids and nanoparticles*; Reaserch Studies Press Ltd.: Philadelphia, PA, 2003.
(28) Venermo, J.; Sihvola, A. *J. Electrost.* **2005**, *63*, 101.

NL900423G